Synthetic Metals 210 (2015) 192–200

Contents lists available at ScienceDirect

Synthetic Metals

journal homepage: www.elsevier.com/locate/synmet

Trans–cis isomerization assisted synthesis of solution-processable yellow fluorescent maleic anhydrides for white-light generation

Mehmet Ozdemir[a], Sinan Genc[b], Resul Ozdemir[a], Yemliha Altintas[a], Murat Citir[a], Unal Sen[c], Evren Mutlugun[b,*], Hakan Usta[a,*]

[a] Department of Materials Science and Nanotechnology Engineering, Abdullah Gül University, Kayseri, Turkey
[b] Department of Electrical and Electronics Engineering, Abdullah Gül University, Kayseri, Turkey
[c] Department of Mechanical Engineering, Abdullah Gül University, Kayseri, Turkey

ARTICLE INFO

Article history:
Received 31 July 2015
Received in revised form 24 September 2015
Accepted 29 September 2015
Available online 29 October 2015

Keywords:
Maleic anhydride
Trans-to-cis isomerization synthesis
White light emitting diode (WLED)
Wavelength-upconverting material

ABSTRACT

Heterocyclic maleic anhydride derivatives have been extensively studied in natural products chemistry over the past few decades. However, their incorporation into optoelectronic devices has lagged behind that of other π-conjugated systems, and they have never been studied in white light emitting diodes (WLEDs). The development of emissive π-conjugated materials for (WLEDs) has been an emerging scientific and technological research area to replace phosphors used in LED-based solid-state lighting. Here, we demonstrate the design, synthesis and characterization of two new highly emissive alkyl-substituted bis(thienyl)maleic anhydrides (C6-Th2MA and C12-Th2MA) with favorable photophysical properties. The new core is synthesized via a novel *trans-to-cis isomerization*-assisted one-pot reaction, which is demonstrated for the first time in the literature for the synthesis of a bis(heteroaryl)maleic anhydride. Due to its favorable absorption and fluorescence properties in the blue and yellow region of the visible spectrum, respectively, C12-Th2MA is studied as a potential wavelength-upconverting material. A WLED fabricated by drop-casting a polymeric solution of C12-Th2MA on a blue LED (InGaN, 455 nm) yields promising CIE coordinates and color-rendering index (CRI) values of (0.24, 0.20) and 65.0, respectively. Considering the simplicity of the current molecular structure and facile synthesis, alkyl-substituted bis(thienyl)maleic anhydrides stand as ideal phosphor alternatives. Therefore, the current findings may open new perspectives for the development of maleic anhydride-based small molecules for low-cost, energy-efficient, and solution-processed lighting technologies.

1. Introduction

Heterocyclic maleic anhydride compounds and their corresponding maleimide derivatives exist in the chemical structure of various natural products and synthetic compounds such as rebeccamycin [1], camphorataanhydride A [2], and camphoratai-mides B and C (Fig. 1) [3–6]. They have been used as amino protecting groups in the synthesis of various natural products including peptides, penicillin derivatives, and oligosaccharides, thanks to their facile and chemoselective protection/deprotection-reactions [7]. Additionally, their highly fluorescent characteristics make them suitable for chromatography-based chiral amine seperations and quantitative measurements [8,9]. When compared with conventional amino protecting groups, their increased volume is advantegeous for further modification into more reactive protecting functionalities. On the other hand, more recently 3,4-bis(heteroaryl)maleic anhydride compounds and their N-substituted maleimide derivatives (e.g., angiogenesis inhibitor Fig. 1), have attracted attention in cancer research due to their antiproliferative activity [10,11]. The *cis*-orientation of the two aromatic rings in a conformationally restricted (*cis*-locked) design allows this type of molecular systems to function as anti-cancer agents. In addition, since they are very resistant to isomerization into their inactive *trans*-forms, they exhibit good stability during prolonged storage. Another promising application of 3,4-bis(heteroaryl)maleic anhydride is photochromism for optical data recording and storage. For this particular application, maleic anhydride/maleimide acts as a favorable *cis*-ethylene bridge between two photocyclizable heterocycles, and they offer the advantages of thermal irreversibility and high cycling number [12,13,14]. Despite all these aforementioned research efforts and advances on bis(heteroaryl)maleic anhydrides in various fields,

* Corresponding authors.
E-mail addresses: evren.mutlugun@agu.edu.tr (E. Mutlugun), hakan.usta@agu.edu.tr (H. Usta).

http://dx.doi.org/10.1016/j.synthmet.2015.09.027
0379-6779/

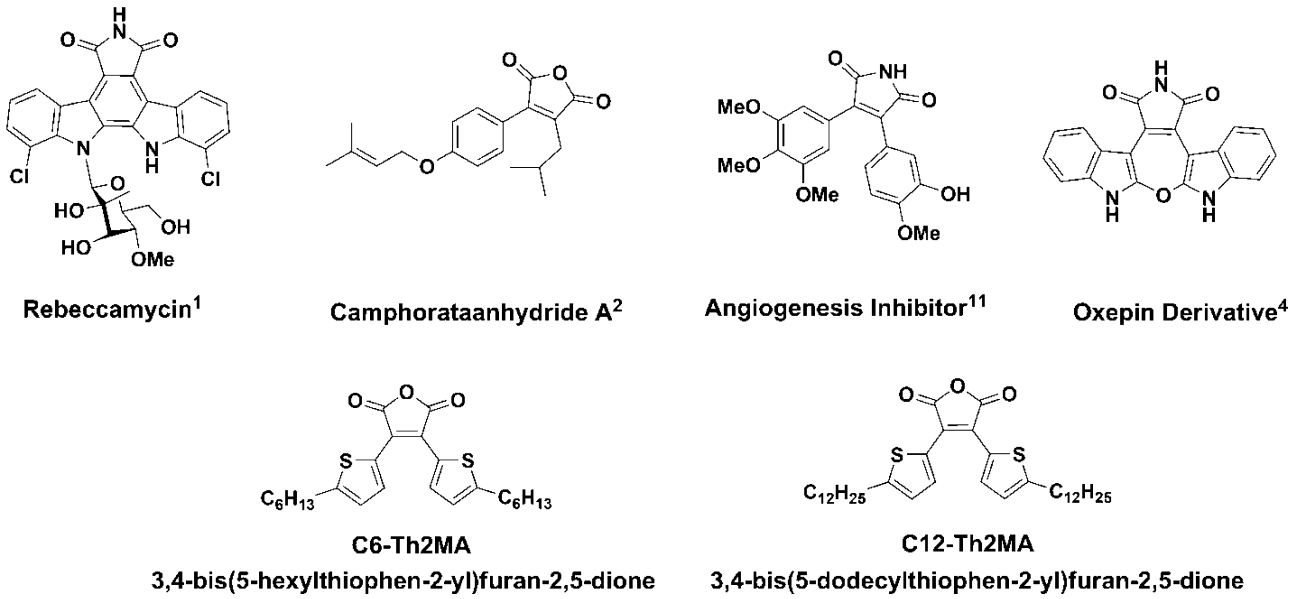

Fig. 1. Chemical structures of some natural and synthetic products based on heteroaryl-substituted maleic anhydrides/maleimides, and **C6-Th2MA** and **C12-Th2MA** developed in this study.

they have been rarely studied for optoelectronic applications. This is quite surprising since some of their derivatives have been discovered to be highly fluorescent. Considering the molecular size and the extent of π-conjugation in bis(heteroaryl)maleic anhydrides, their absorption and emissive characteristics might be effectively coupled with the higher energy complementary emissive systems (i.e., blue LEDs) to achieve white light. Solid-state lighting and display applications based on white light-emitting devices (WLEDs) have gained significant scientific and technological importance over the past few decades due to their high luminous efficiency, energy efficiency, reliability, long lifetime, and low toxicity [15,16]. They are considered to be ideal replacements of conventional incandescent and mercury-containing fluorescent lights in the near future [17]. Among various strategies employed in WLEDs available on the market today, the majority relies on blue-emitting GaN LEDs (450–470 nm) coated with yellow-emitting $Y_3Al_5O_{12}:Ce^{3+}$(YAG:Ce^{3+}) phosphor. Recently, hybrid organic–inorganic emissive systems have demonstrated great promise due to their highly tunable optical properties, high light quality and facile fabrication of organic systems. To this end, as blue and yellow are almost exactly complementary [18], we envision that solution-processed organic films based on yellow emissive bis(heteroaryl)maleic anhyride compounds might be effectively coupled with the proper blue inorganic-based LEDs to achieve white light. Based on pre-synthesis computational modeling, we proposed 2-alkylthienyl subtituted maleic anhyride derivatives as promising agents for white light generation. It is noteworthy that, to the best of our knowledge, among the few diaryl-substituted maleic anhydride derivatives studied to date, alkyl substituted thienyl derivatives have never been reported in the literature, and their fluorescent behaviors in light-emitting applications have never been studied.

In this report, with the motivation of extending the knowledge on the synthesis of heteroarylmaleic anhydride derivatives and exploring their potential in light-emitting applications,we demonstrate the theoretical design, *trans-to-cis* isomerization assisted synthesis, photophysical properties and the preliminary white-light emissive characteristics of two new compounds, **C6-Th2MA** and **C12-Th2MA**, with lipophilic hexyl (-*n*-C_6H_{13}) and dodecyl (-*n*-$C_{12}H_{25}$) substituents, respectively (Fig. 1). In these compounds, thiophenes are attached from their 2 positions to maleic anhydride's 3 and 4 positions to maximize the π-conjugation length. Alkyl chains of hexyl (-*n*-C_6H_{13}), and dodecyl (-*n*-$C_{12}H_{25}$) substituents are located at molecular termini to provide sufficient solubility for the synthesis, purification and device processing. In addition, lipophilic alkyl substituents can impede proper intermolecular π–π stacking and thus lower the possibility of undesired intermolecular energy/charge transfers and excimer formation [19]. The key step in the current synthesis is a one-pot reaction, which include successive steps of "*alkaline hydrolysis*", "*acid-catalyzed trans-to-cis isomerization*", and "*anhydride formation*" in appreciable yields (40–50%). To date, most of the synthetic routes toward bis(heteroaaryl)maleic anhydrides have focused on either consecutive condensation reactions of non-cyclic building blocks or cross-coupling reactions of dihalogenated maleic anhydride/maleimide derivatives [20–22]. To the best of our knowledge, this reaction is the first example of an *trans-to-cis* isomerization-based synthesis of diaryl-substituted maleic anhydrides, and it may open doors to the realization of new derivatives. The new compound absorbs blue light (λ_{max} = 455 nm) and emits yellow light (λ_{max} = 570 nm) in the solid-state, and the fluorescence quantum yield (Φ_f) is calculated as 0.35 in *n*-hexane. A WLED assembly was built on a blue-emitting LED chip (InGaN, 455 nm) by hybridizing with a polymethylmethacrylate (PMMA) solution (500 mg/ml) in DMF doped with 0.7 wt.% of C12-Th2MA. The Commission International de l'Eclairage (CIE) coordinates and color-rendering index (CRI) values are found to be (0.24, 0.20) and 65.0, respectively, indicating that alkyl-substituted bis(thienyl)maleic anhydride derivatives are ideal phosphor alternatives for solid-state lighting applications. Considering the simplicity of the current molecular structures and facile synthesis, the maleic anhydride-based π-conjugated emitters may open new perspectives for the realization of low-cost, energy-efficient, and solution-processed lighting technologies.

2. Results and discussions

2.1. Pre-synthesis computational modeling

In the pre-synthesis computational modeling, the optimization of the molecular geometries and total energy calculations were carried out using density functional theory (DFT) at the B3LYP/6-31G** level. While the molecular structure of the target

compounds **1** and **2** were illustrated by the model compound **M2**, **M1** represents the structurally related reference fluorescent probe "*N*-methyl 2,3-diphenylmaleimide" (Fig. 2) [23]. Since **M1** is known to exhibit a green fluorescence at λ_{em}^{max} = 506 nm, in order to transform the green emission of **M1** to a desired yellow–orange emission, HOMO–LUMO energy gap reduction of 0.5–1.0 eV is desired with the model compound **M2**. However, this design requires a delicate balance between a good optical absorption in the blue region (λ_{abs}^{max} = 450–495 nm) and emission in the yellow region (λ_{em}^{max} = 570–590 nm) of the visible spectrum.

As shown in Fig. 2, the HOMO–LUMO gap for the model compound **M2** is found to be 0.8 eV lower than that of the reference compound **M1** as a result of concurrent increase in the HOMO level and decrease in the LUMO level. In both cases, while HOMO is found to be highly delocalized along the aryl-ethylene-aryl moiety, LUMO is found to be mostly localized on the maleic anhydride acceptor part with a relatively small contribution from the donor aryl units. Such dependence of LUMO on acceptor unit and HOMO on the donor unit is very typical for donor–acceptor systems, and it indicates that HOMO–LUMO excitations may be associated with partial/complete charge separations [24]. Therefore, the absorption and emission profiles of the new compounds are expected to show solvachromatism, which is consistent with our photophysical characterizations (vide infra).

While the HOMO electron density distributions of **M1** and **M2** are mostly identical, the LUMO electron density distribution of **M2** system has significantly higher contribution from the thiophene units compared to that of **M1**, which indicates an enhanced π-delocalization, and therefore, more stabilized LUMO energy level. The differences between **M1** and **M2** frontier orbital energy levels reflect both the effects of the π electron-donating S atom versus simple —C=C— and the more planar conformation of five–five (torsion angle ~19°) versus five–six (torsion angle ~37°) interring linkages between maleic anhydride and aryl units (Fig. S1) [25]. In addition, the simulated absorption profile of the model target compound **M2** indicates a red-shifted absorption maxima ($\Delta\lambda_{max}$ = +60 nm) compared to that of green-emissive reference compound **M1** (Fig. S1). This wavelength shift should be ideal to transform the absorption characteristics of the new molecules into the blue absorbing region, as well as the corresponding emission to yellow–orange region. It is noteworthy that although real peak positions and Stokes shifts depend on the molecular environment in solid-state, theoretical results clearly indicates that the new 3,4-bis(5-alkylthiophen-2-yl)maleic anhydride systems are most likely to absorb in the blue region and emit in the yellow–orange region, which is favorable for the fabrication of WLEDs. The pre-synthesis theoretical results prompted us to synthesize these new derivatives and characterize them for white light generation.

2.2. Synthesis and characterizations

As shown in Scheme 1, compounds **C6-Th2MA** and **C12-Th2MA** were prepared from commercially available thiophene in four steps. Thiophene is first lithiated with *n*-butyllithium and subsequently reacted with 1-bromohexane and 1-bromododecane to give 2-hexylthiophene (**1a**) (56% yield) and 2-dodecylthiophene (**1b**) (83% yield), respectively. The corresponding trimethylstannane compounds (5-hexylthiophen-2-yl) trimethylstannane (**2a**) and (5-dodecylthiophen-2-yl) trimethylstannane (**2b**) were synthesized from **1a** and **1b** via lithitation/stannylation reactions with 93% and 63% yields, respectively. Then, Stille coupling of **2a** and **2b** with dimethyl 2,3-dibromofumarate yields dimethyl 2,3-bis(5-hexylthiophen-2-yl)fumarate (**3a**) and dimethyl 2,3-bis(5-dodecylthiophen-2-yl)fumarate (**3b**), respectively in very high yields of 92–93%. In this particular coupling reaction, bis(triphenylphosphine)palladium(II) dichloride/THF is found to be the best catalyst/solvent system and the reaction time is found to be very critical to maximize the product yield. While 48 h of reaction time is required to achieve yields of more than 90%, lower reaction yields (<50%) with significant amount of mono-coupled intermediate were observed when the reaction is stopped between 6 and

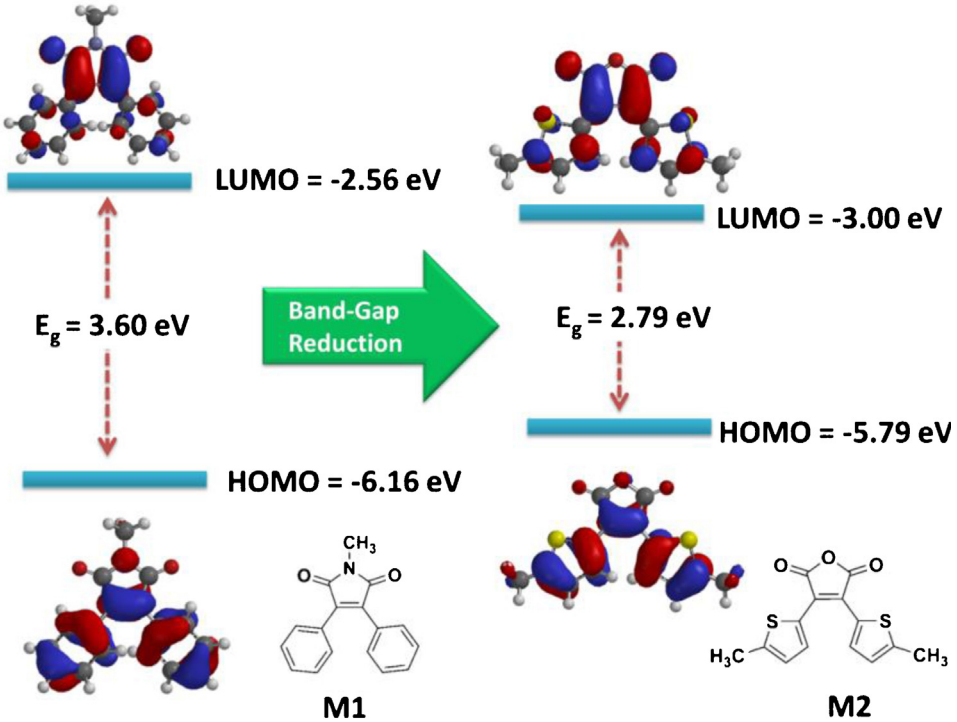

Fig. 2. Computed HOMO and LUMO energy levels and topographical representations of the reference compound, *N*-methyl 2,3-diphenylmaleimide (**M1**) and the model compound, 3,4-bis(5-methylthiophen-2-yl)maleic anhyride (**M2**) (DFT, B3LYP/6-31G**).

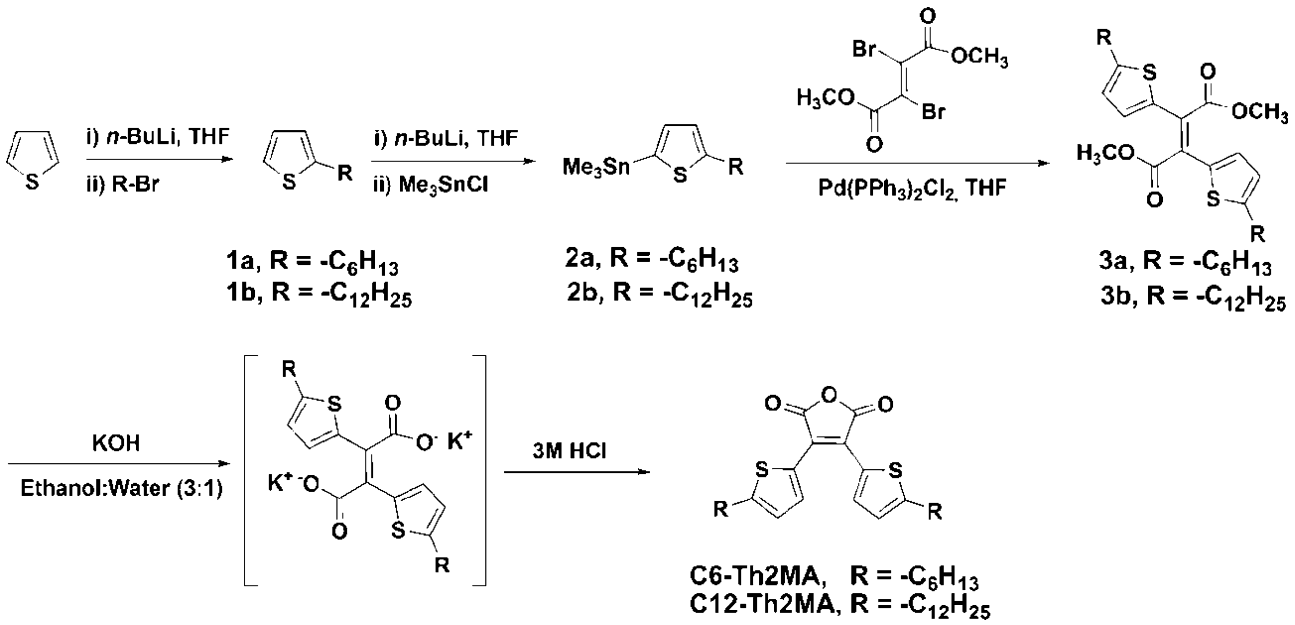

Scheme 1. Synthesis of compounds **C6-Th2MA** (3,4-bis(5-hexylthiophen-2-yl)furan-2,5-dione) and **C12-Th2MA** (3,4-bis(5-dodecylthiophen-2-yl)furan-2,5-dione).

24 h. This double cross-coupling reaction is monitored by TLC, and the limiting reagent, dimethyl 2,3-dibromofumarate, is found to disappear in the first 6 h forming mostly mono-coupled intermediate. However, it takes another 42 h to convert all of the mono-coupled product to the desired bis-coupled **3a** and **3b**, which indicates kinetically less reactive nature of the mono-coupled product after thiophene addition. In the final step, compounds **3a** and **3b** are first hydrolyzed in ethanol:water mixture with KOH via alkaline saponification method, and then acidified. Treatment of the hydrolysis reaction mixture with 3 M HCl is found to induce consequtive steps of neutralization, *trans–cis* isomerization, and anhydride formation, yielding the target maleic anhydride compounds **C6-Th2MA** and **C12-Th2MA** in 40% and 50% yields, respectively. The acid treatment was performed both directly on the hydrolysis mixture after the saponification reaction, and also on the isolated hydrolysis solid which was isolated from the saponification mixture directly after hydrolysis reaction. In both cases, target compounds **C6-Th2MA** and **C12-Th2MA** are obtained in comparable yields. The new compounds are very soluble in common organic solvents ($CHCl_3$, CH_2Cl_2, THF, and toluene), which allows convenient purification by flash column chromatography. The intermediate and final compounds' chemical structures and purities are verified by $^1H/^{13}C$ NMR spectroscopy (Fig. S1–S8), elemental analysis, and IR.

Our approach to prepare **C6-Th2MA** and **C12-Th2MA** involved a key *trans-to-cis* isomerization reaction, in which consequtive steps of saponification, *trans-to-cis* isomerization, and intramolecular anhydride formation occurred in one-pot. Although *cis-to-trans* isomerization reaction is known for the benchmark conversion of maleic acid to fumaric acid, *trans-to-cis* conversion for diaryl-substituted fumarates is reported here for the first time in the literature. It appears that the further intramolecular cyclic anhydride formation plays a key role to drive this reaction. Note that we were unable to isolate *trans*-dicarboxylic acid, even when exact equivalence of H^+ is added (2.0 equiv.) during acidification, which is expected to only neutralize the carboxylate functionalities. In this case, isomerization still occured and followed by anhydride formation, which indicates that even a catalytic amount of H^+ is sufficient to promote isomerization/cyclization. This is consistent with the previous reports on similar anhyride formations from *cis*-dicarboxylates [20]. The plausible mechanism for the acid-catalyzed *trans-to-cis* isomerization is depicted in Fig. 3. When the alkaline hydrolysis product having two carboxylates is acidified, the carboxylate groups are first neutralized with the

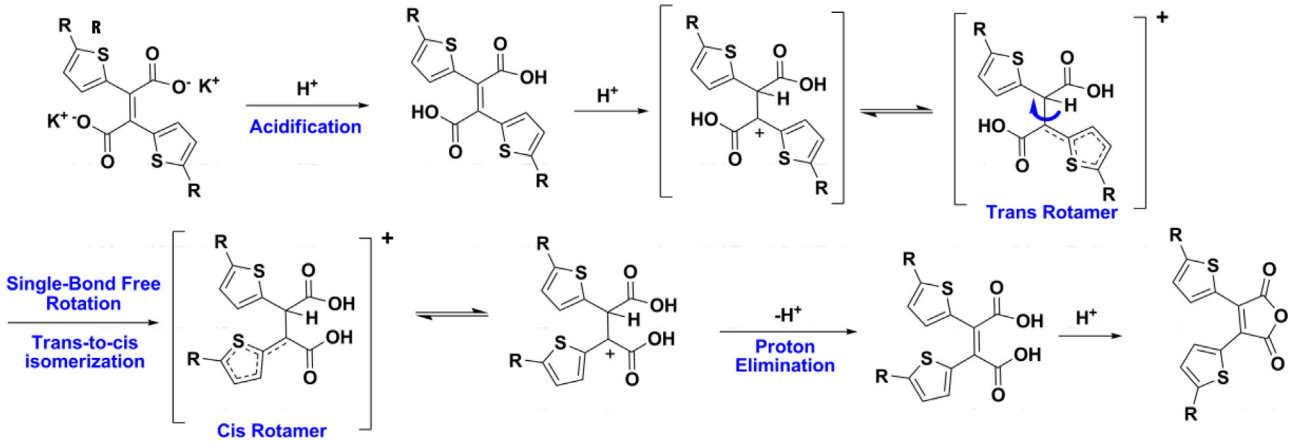

Fig. 3. The proposed mechanism for acid-catalyzed *trans-to-cis* isomerization of dimethyl 2,3-bis(5-alkylthiophen-2-yl)fumarate to yield maleic anhydride compound.

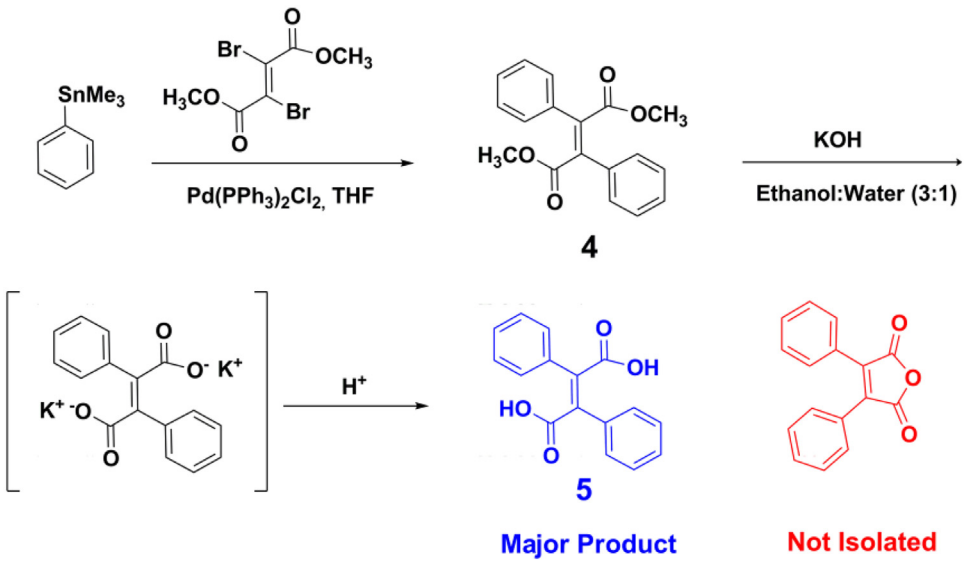

Scheme 2. The synthesis and alkaline hydrolysis/acidification step of dimethyl 2,3-diphenylfumarate (**4**) yielding dicarboxylic acid compound 2,3-diphenylfumaric acid (**5**).

initial two equivalence of H^+ to form a diacid, which undergoes a protonation from the ethylene carbon site forming a *trans*-carbonium intermediate. The free rotation of the C3—C4 bond of the *trans*-carbonium yields *cis*-carbonium ion immediately, which can be also further stabilized by intramolecular hydrogen bonds. This carbonium intermediates can be effectively stabilized with the neighboring π-electron-rich thiophene moiety through resonance delocalizations and inductive effects. In the final step, proton elimination and anhydride formation yields the final desired compounds. Similar acid-catalyzed isomerization mechanisms were previously reported for *cis*-1-phenyl-1,3-butadiene and *cis*-1-methyl-3-phenylallyl alcohol compounds [26]. However, we should note that detailed kinetic/thermodynamic studies are needed to fully identify these steps.

To better understand the synthetic utility and scope of this methodology, we explored the reaction of 2,3-diphenylfumarate (**4**) through a similar saponification/acidification method. First, **4** was synthesized via Stille coupling of phenyltrimethylstannane with dimethyl 2,3-dibromofumarate in very high yield of 93%. Similar to thienyl-substituted coupling reactions, bis(triphenylphosphine)palladium(II) dichloride/THF is found to be the best catalyst/solvent system and the reaction time is found to be very critical to maximize the product yield. Upon acidification of the hydrolyzed intermediate, 2,3-diphenylfumarate, only dicarboxylic acid compound, 2,3-diphenylfumaric acid (**5**), is isolated with no maleic anhydride compound formation (Scheme 2). Therefore, it appears that this isomerization reaction is very sensitive to the nature of aryl unit, and thiophene exhibits favorable structural and electronic effects for this particular methodology. This may be attributed to two different effects based on the mechanism proposed: (i) sterically more encumbered nature of the six-membered benzene ring versus five-membered thiophene ring makes the *trans-to-cis* isomerization sterically more demanding, (ii) the carbonium intermediate formed during the isomerization reaction is stabilized more favorably with the neighboring π-electron-rich thiophene moiety through resonance delocalizations and inductive effects compared to benzene ring. Further studies to fully explore the scope of this methodology on various five-membered heteroaryl units are undergoing and will be reported accordingly.

2.3. Photophysical properties and white light generation

C12-Th2MA is used as a wavelength-upconverting material for WLED applications, based on its robust solid form at room temperature. First, solution-based optical absorption and

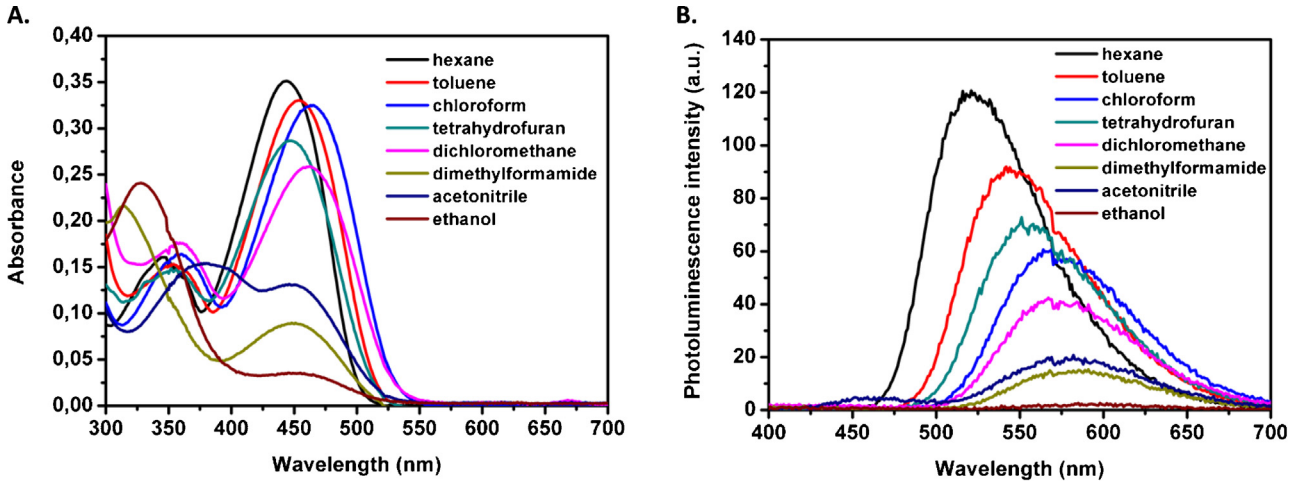

Fig. 4. (a) The optical absorption and (b) photoluminescence spectra of C12-Th2MA in different solvents.

Table 1
The optical absorption and photoluminescence emission peaks, Stokes shifts amplitudes, and quantum yields of C12-Th2MA in different solvents.

	Hexanes (ε = 1.9)	Toluene (ε = 2.4)	$CHCl_3$ (ε = 4.8)	THF (ε = 7.6)	CH_2Cl_2 (ε = 8.9)	DMF (ε = 36.7)	Acetonitrile (ε = 37.5)	Ethanol (ε = 24.5)
λ_{abs}^{max} (nm)	446	454	463	448	461	450	451	458
λ_{em}^{max} (nm)	521	545	554	571	577	580	587	596
Stokes Shifts (nm)	77	91	91	123	116	130	136	138
Φ_f	0.35	0.33	0.21	0.24	0.14	0.07	0.09	0.008

photoluminescence characterizations were performed by preparing its dilute solutions (2.1×10^{-5} M) in various solvents (hexane, toluene, chloroform, tetrafhydrofuran, dichloromethane, dimethylformamide, acetonitrile and acetone) with different dielectric constants.

The spectra are shown in Fig. 4 and the optical data are presented in Table 1. Although the trends are slightly different, both absorption and emission profiles exhibit positive solvachromatisms. As expected from the pre-synthesis theoretical modeling, absorption maxima are located in the blue region (446–463 nm) of the visible spectrum, and match perfectly with the calculated HOMO–LUMO gap of 2.79 eV (444 nm). On the other hand, yellow emission (571–596 nm) is observed in relatively polar solvents and as well as in the solid-state (Fig. 6). In the fluorescence spectra, a clear red-shift in the emission maxima has been observed from 521 nm to 596 nm as the solvent polarity increases (*n*-hexane (ε = 1.9) → $CHCl_3$ (ε = 4.8) → THF (ε = 7.6) → ethanol (ε = 24.5) [27]. A similar trend was also observed in the absorption profile with a smaller red-shift (~19 nm) of the excitonic peak. The presence of red-shifts in both absorption and emission profiles suggests that the Franck–Condon excited state ($S_1(\pi-\pi^*)$) has a significant polar character as a result of charge seperation induced by photoexcitation [28]. The observed larger red-shift in the fluorescence profile ($\Delta\lambda$ = 75 nm) compared to that in the absorption profile ($\Delta\lambda$ = 19 nm) indicates that the dipole moment is larger in the final relaxed excited state than in the ground state. These observations are in line with the computational results that HOMO to LUMO excitations may yield partial or complete charge-transfers.

The fluorescence quantum yield (Φ_f) of C12-Th2MA in different solvents was calculated using a reference dye, quinine sulphate, which has a known quantum efficiency of 0.577 in 0.1 M H_2SO_4 (excited using 350 nm monochromatic light) [29]. The emission quantum efficiency of the C12-Th2MA in various solvents was calculated using the following equation:

$$QE_{C12} = QE_{Std} \times \left(\frac{I_{C12}}{I_{Std}}\right) \times \left(\frac{A_{Std}}{A_{C12}}\right) \times \left(\frac{n_{C12}}{n_{Std}}\right)^2 \quad (1)$$

where QE_{Std} and QE_{C12} are the quantum efficiency of the standard quinine sulphate and synthesized C12-Th2MA; *I* is the integrated emission peak areas of the C12-Th2MA and the standard; *A* is the absorbance value at excitation wavelength of 350 nm; *n* is the refractive index of the solvent of the standard sample and C12-Th2MA. The quantum yield is found to be the highest in relatively non-polar *n*-hexane, and it gradually decreases with increasing the solvent polarity (0.35 in hexane (ε = 1.9) → 0.008 in ethanol (ε = 24.6)). This decrease in quantum yield correlates well with the increased Stokes shift amplitudes from *n*-hexane (~77 nm) to ethanol (~138 nm). These results are consistent with the general fact that larger Stokes shift amplitudes indicates longer excited-state lifetimes and increases the relative probability of non-radiative decay, and thus decreases the PL quantum efficiencies [30]. This suggests that the higher polarity solvents facilitates intra-/inter-molecular charge-transfers via stabilization of the polarized excited state products, which result in large Stokes shifts and fluorescence quenching [31]. The quantum efficiency obtained for the new molecule is in the range of yellow-emitting iridium complex [32], and lower than that of the benchmark phosphor color converter, yttrium aluminum garnet (YAG) doped with cerium (Ce), YAG:Ce ($Y_3Al_5O_{12}:Ce^{3+}$) ($\Phi > 0.85$), which has been extensively used for solid state lighting applications [33]. Although this reflects the difference in the nature of the emissions (triplet-state emission of phosphors versus singlet-state emission of small molecules), the fact that rare-earth elements are not needed in the new fluorescent small molecules makes them quite attractive for sustainable white light generation [34]. Fig. 5 shows the intensities of photoluminescence excitation (PLE) spectra of C12-Th2MA in different solvents monitored at the corresponding emission maxima in the yellow region of the visible spectrum. Although varies slightly based on the solvent, excitation maxima of ~460–470 nm are observed, which matches well with the emission profile of the blue-emitting LED chips (450–470 nm).

After observing the favorable blue absorbing and yellow emitting characteristics, the new molecule has been studied as a potential wavelength-upconverting material for generating white light. For decades, commercially available phosphorous materials have been used in conjunction with the blue LEDs to develop white light, which has recently emerged in home electronics for LCD backlights and as white illuminants. Today, the most widely used WLEDs include a yellow-emitting $Y_3Al_5O_{12}:Ce^{3+}$(YAG:Ce^{3+}) phosphor integrated to a blue-emitting LED. However, the shortage on the supply of rare earth elements has led to research efforts to replace phosphor with affordable counterparts [34]. In this regards, solution-processable, potentially low-cost organic small molecules, such as C12-Th2MA, which can be synthesized in few steps, stand as promising phosphor alternatives.

In order to achieve white light emission, two color mixing approach of blue and yellow colors is used. Upon screening the

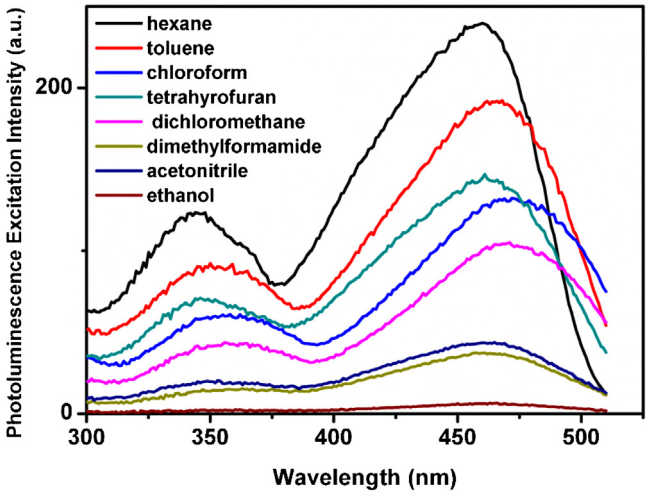

Fig. 5. Photoluminescence excitation (PLE) spectra of C12-Th2MA obtained by monitoring the intensity of the corresponding emissions at peak emission wavelengths associated with different solvents.

concentration of yellow-emitting material in the film, the most optimized white light spectral composition for the best achievable CRI is identified for 0.7 wt.% of C12-Th2MA in polymethylmethacrylate (PMMA) solution in DMF (500 mg/ml). This viscous solution is drop-casted on a commercially available blue LED chip (InGaN, 455 nm), which has been driven at 2.6 V. A bright white light is achieved (Fig. 6B) in the device on-state, and the output light has been collected with a spectrometer resulting in an overall electroluminescence (EL) spectrum shown in Fig. 6. The EL spectrum contains two distinct emission bands at ~455 nm and ~570 nm, where the short-wavelength peak is directly from the underlying LED chip, and the broad long-wavelength peak originates from the emission of C12-Th2MA in the solid-state upon the absorption of blue light. The figures of merits of the white light, i.e., color coordinates and the color rendering index have been calculated based on the electroluminescence spectrum obtained. Color rendering index (CRI) is one of the most widely used metrics to calculate color rendering capability of the illuminants (CIE, 1971). The ability of a light source to render the color is calculated upon comparison with that of a reference light source. For the calculation of general CRI, special CRI sets are used.

$$\mathrm{CRI}_{\mathrm{general}} = \frac{1}{8}\sum_{i=1}^{8}\mathrm{CRi}_i \quad (2)$$

Color rendering indices are calculated according to

$$\mathrm{CRI}_i = 100 - 4.6\Delta E_i^* \quad (3)$$

where ΔE_i^* stands for the quantitative measure of the color change due to the illumination with the test source and reference source [35]. CRI equals to 100 when the illumination source is identical to that of a blackbody radiator. Carrying out the calculations; we have achieved the coordinates of the white light as (0.24, 0.20) falling in the shades of bluish white light, and calculated the color rendering index as 65.0. This characteristic of bluish white light is more suitable for applications to give the perception of light required in exhibition activities (i.e., museum or gallery), and recently for backlighting in displays, as demonstrated in a recent study with coordinates of (*x*, *y*) (0.24, 0.21) [36]. In addition, the bluish white light is crucial to specifically stimulate the retina cells, which directly drives the human biological clock for daily alertness, and thus, bluish white light is an important component of lighting. It is noteworthy that the pure white light (0.33, 0.33) can be achieved via adding a third red component as shown in the literature for other yellow emitting materials [37]. An accelerated luminescence test is performed on the films of C12-Th2MA under constant blue light illumination ($\lambda_{\mathrm{exc.}}$ = 455 nm) to observe any change in the luminescence property. Based on this experiment, the films were found to remain around 80% of their initial peak intensity after 5 h of testing (Fig. S2). Although this result shows a good stability of this new material, it is noteworthy that for industrial applications, a careful optimization of LED heat sink and remote phosphor approach may be needed to further enhance the stability. The generation of white light using maleic anhydride derivatives has been shown for the first time in the literature with promising color performances.

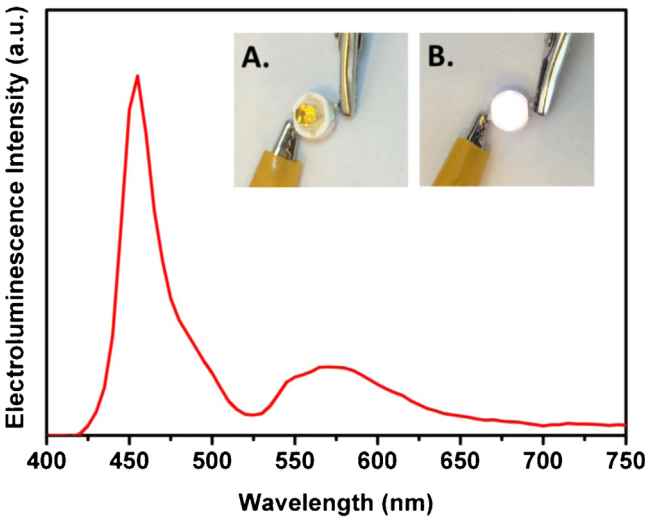

Fig. 6. The room temperature electroluminescence spectrum of WLED fabricated by drop-casting 0.7 wt.% of C12-Th2MA in polymethylmethacrylate (PMMA) solution (yellow coating in (A)) on a blue-emitting LED (InGaN, 455 nm). Photographs of the WLED assemblies before (A) and after (B) the device is turned on (2.6 V).

3. Conclusions

In summary, two new highly emissive alkyl-substituted bis (thienyl)maleic anhydride compounds, C6-Th2MA and C12-Th2MA, has been designed, synthesized, and characterized. The new compounds are end-functionalized with lipophilic alkyl substituents (-*n*-C_6H_{13} and -*n*-$C_{12}H_{25}$) to provide sufficient solubility for the synthesis/purification and device processing, and also to enhance solid-state fluorescence. Different than the previously reported methodologies, the key step is a one-pot reaction, which include successive steps of "*alkaline hydrolysis*", "*acid-catalyzed trans-to-cis isomerization*", and "*anhydride formation*" in appreciable yields (40–50%). To the best of our knowledge, this reaction is the first example of a "*trans-to-cis* isomerization"-based synthesis of diaryl-substituted maleic anhydride core, and it may lead to the realization of new derivatives. C12-Th2MA is found to absorb blue light (λ_{max} = 455 nm) and emit yellow light (λ_{max} = 570 nm) in the solid-state, and the fluorescence quantum yield (Φ_f) is calculated as 0.35 in *n*-hexane, which makes this molecule suitable for wavelength-upconversion. A WLED is fabricated on a blue LED (InGaN, 455 nm) by drop-casting a polymeric solution of C12-Th2MA, which yields promising CIE coordinates and CRI values of (0.24, 0.20) and 65.0, respectively. The promising photophysical properties and WLED performance presented in this study indicates that bis(heteroaryl)maleic anhydrides are ideal phosphor alternatives for white light generation. The reasonably simple molecular structure and facile synthesis will pave the way for the realization of low-cost and solution-processable LED-based solid-state lighting technologies.

4. Experimental

4.1. Materials and methods

All reagents were purchased from commercial sources and used without further purification unless otherwise noted. Conventional Schlenk techniques were used, and reactions were carried out under N_2 unless otherwise noted. NMR spectra were recorded on a Bruker 400 spectrometer (^{1}H, 400 MHz; ^{13}C, 100 MHz). Elemental analyses were performed by Midwest Microlab, LLC (Indiana, USA).

4.2. Synthesis and characterizations

4.2.1. Synthesis of 2-hexylthiophene (1a)

To a stirred solution of thiophene (2.0 g, 23.81 mmol) in anhydrous THF (10 ml) at −78 °C, *n*-BuLi (2.5 M in hexane, 9.5 ml, 23.81 mmol) was added dropwise over 20 min. The reaction

mixture was stirred at room temperature for 1 h and then cooled to −78 °C. Then, 1-bromohexane (4.32 g, 26.19 mmol) was added dropwise to this solution at −78 °C. The reaction mixture was allowed to warm slowly to room temperature and stirred at room temperature for 16 h. Then, the reaction mixture was slowly poured into water, and the product was extracted with hexanes. The organic layer was dried over Na_2SO_4, filtrated, and evaporated. The crude product was purified by flash column chromatography on silica gel using hexanes as the eluent to give 2-hexylthiophene as a colorless oil (2.23 g, 56% yield). ^{1}H NMR (400 MHz, $CDCl_3$) δ 7.11 (d, 1H, J = 5.2 Hz), 6.94 (dd, 1H, J = 5.2 Hz, J = 4.0 Hz), 6.80 (d, 1H, J = 4.0 Hz), 2.85 (t, 2H, J = 8.0 Hz), 1.71 (m, 2H), 1.30–1.39 (m, 6H), 0.92 (t, 3H, J = 7.0 Hz).

4.2.2. Synthesis of 2-dodecylthiophene (1b)

To a stirred solution of thiophene (2.0 g, 23.81 mmol) in anhydrous THF (10 ml) at −78 °C, *n*-BuLi (2.5 M in hexane, 9.5 ml, 23.81 mmol) was added dropwise over 20 min. The reaction mixture was stirred at room temperature for 1 h and then cooled to −78 °C. Then, 1-bromododecane (6.53 g, 26.19 mmol) was added dropwise to this solution at −78 °C. The reaction mixture was allowed to warm slowly to room temperature and stirred at room temperature for 16 h. Then, the reaction mixture was slowly poured into water, and the product was extracted with hexanes. The organic layer was dried over Na_2SO_4, filtrated, and evaporated. The crude product was purified by column chromatography on silica gel using hexanes as the eluent to give 2-dodecylthiophene as a colorless oil (6.01 g, 83% yield). ^{1}H NMR (400 MHz, $CDCl_3$) δ 7.11 (d, 1H, J = 5.2 Hz), 6.93 (dd, 1H, J = 5.2 Hz, J = 4.0 Hz), 6.79 (d, 1H, J = 4.0 Hz), 2.84 (t, 2H, J = 8.0 Hz), 1.69 (m, 2H), 1.28–1.38 (m, 18H), 0.90 (t, 3H, J = 7.0 Hz).

4.2.3. Synthesis of (5-hexylthiophen-2-yl) trimethylstannane (2a)

To a solution of 2-hexylthiophene (2.3 g, 13.85 mmol) in anhydrous THF (15 ml) at −78 °C, *n*-BuLi (6.1 ml, 15.24 mmol; 2.5 M in hexane) was added dropwise over 20 min. The reaction mixture was heated to room temperature and stirred at this temperature for 1 h, and then cooled again back to −78 °C. Trimethyltinchloride (3.17 g, 15.93 mmol) was added as a solid under positive nitrogen flow, and the resulting mixture was allowed to warm slowly to ambient temperature overnight. The reaction mixture was quenched with water and extracted with hexanes. The organic phase was dried with Na_2SO_4, filtrated, and evaporated to dryness to yield (5-hexylthiophen-2-yl) trimethylstannane as a pale yellow liquid (4.28 g, 93% yield). ^{1}H NMR (400 MHz, $CDCl_3$) δ 7.03 (d, 1H, J = 4.0 Hz), 6.91 (d, 1H, J = 4.0 Hz), 2.87 (t, 2H, J = 8.0 Hz), 1.70 (m, 2H), 1.30–1.39 (m, 6H), 0.92 (t, 3H, J = 7.0 Hz), 0.35 (s, 9H).

4.2.4. Synthesis of (5-dodecylthiophen-2-yl) trimethylstannane (2b)

To a solution of 2-dodecylthiophene (2.0 g, 7.92 mmol) in anhydrous THF (20 ml) at −78 °C, *n*-BuLi (3.48 ml, 8.71 mmol; 2.5 M in hexane) was added dropwise over 20 min. The reaction mixture was heated to room temperature and stirred at this temperature for 1 h, and then cooled again back to −78 °C. Trimethyltinchloride (1.9 g, 9.5 mmol) was added as a solid under positive nitrogen flow, and the resulting mixture was allowed to warm slowly to ambient temperature overnight. The reaction mixture was quenched with water and extracted with hexanes. The organic phase was dried with Na_2SO_4, filtrated, and evaporated to dryness to give (5-dodecylthiophen-2-yl) trimethylstannane as a colorless liquid (2.06 g, 63 % yield). ^{1}H NMR (400 MHz, $CDCl_3$) δ 7.03 (d, 1H, J = 4.0 Hz), 6.91 (d, 1H, J = 4.0 Hz), 2.87 (t, 2H, J = 8.0 Hz), 1.70 (m, 2H), 1.28–1.41 (m, 18H), 0.90 (t, 3H, J = 7.0 Hz), 0.36 (s, 9H).

4.2.5. Synthesis of dimethyl 2,3-bis(5-hexylthiophen-2-yl)fumarate (3a)

Bis(triphenylphosphine)palladium(II) dichloride (0.075 g, 0.108 mmol) was added to a solution of (5-hexylthiophen-2-yl) trimethylstannane (2 g, 6.04 mmol) and dimethyl 2,3-dibromofumarate (0.65 g, 2.16 mmol) in anhydrous THF (20 ml). The reaction mixture was heated at 110 °C for 2 days. The reaction was followed by thin-layer chromatography. After the reaction is completed, the reaction mixture was concentrated on the rotary evaporator to give a dark crude semi-solid. The crude product was purified by column chromatography on silica gel using dichloromethane as the eluent to give dimethyl 2,3-bis(5-hexylthiophen-2-yl)fumarate as a yellow oil (0.952 g, 92.6% yield). ^{1}H NMR (400 MHz, $CDCl_3$) δ 6.88 (d, 2H, J = 4.0 Hz), 6.71 (d, 2H, J = 4.0 Hz), 3.87 (s, 6H), 2.77 (t, 4H, J = 8.0 Hz), 1.63 (m, 4H), 1.26–1.36 (m, 12H), 0.89 (t, 6H, J = 7.0 Hz). ^{13}C NMR (100 MHz, $CDCl_3$) δ 167.6, 151.8, 132.9, 131.5, 130.5, 124.3, 52.8, 31.5, 31.4, 30.2, 28.7, 22.6, 14.1; anal. calcd. for $C_{26}H_{36}O_4S_2$: C, 65.51; H, 7.61. Found: C, 65.32; H, 7.45.

4.2.6. Synthesis of dimethyl 2,3-bis(5-dodecylthiophen-2-yl)fumarate (3b)

Bis(triphenylphosphine)palladium(II) dichloride (0.069 g, 0.010 mmol) was added to a solution of (5-dodecylthiophen-2-yl) trimethylstannane (2.31 g, 5.56 mmol) and dimethyl 2,3-dibromofumarate (0.60 g, 1.99 mmol) in anhydrous THF (15 ml). The reaction mixture was heated at 110 °C for 2 days. The reaction was followed by thin-layer chromatography. After the reaction is completed, the reaction mixture was concentrated on the rotary evaporator to give a dark crude semi-solid. The crude product was purified by column chromatography on silica gel using dichloromethane as the eluent to give dimethyl 2,3-bis(5-dodecylthiophen-2-yl)fumarate (1.18 g, 91.9% yield). ^{1}H NMR (400 MHz, $CDCl_3$) δ 6.89 (d, 2H, J = 4.0 Hz), 6.71 (d, 2H, J = 4.0 Hz), 3.87 (s, 6H), 2.77 (t, 4H, J = 8.0 Hz), 1.62 (m, 4H), 1.23–1.34 (m, 36H), 0.90 (t, 6H, J = 7.0 Hz); ^{13}C NMR (100 MHz, $CDCl_3$) δ 167.7, 151.9, 132.9, 131.5, 130.6, 124.3, 52.9, 32.0, 31.9, 31.5, 31.4, 30.3, 29.7, 29.4, 29.1, 22.8, 22.7, 14.2, 14.1; anal. calcd. for $C_{38}H_{60}O_4S_2$: C, 70.76; H, 9.38. Found: C, 70.43; H, 9.22; m.p. 74–75 °C.

4.2.7. Synthesis of 3,4-bis(5-hexylthiophen-2-yl)furan-2,5-dione (C6-Th2MA)

A solution of dimethyl 2,3-bis(5-dodecylthiophen-2-yl)fumarate (**3a**) (0.5 g, 1.05 mmol) and potassium hydroxide (1.09 g, 19.4 mmol) in ethanol:water (33:4.5 ml) solvent mixture was refluxed at 105 °C for 16 h. The reaction mixture was then allowed to cool to room temperature, and then acidified to "pH 0–1" by HCl (3 M, 11 ml). The product was extracted from the resulting orange–red mixture by using chloroform. The resulting organic phase was washed with water, dried with Na_2SO_4, filtered, and evaporated to dryness to give a crude product. The crude product was purified by column chromatography on silica gel using chloroform as the eluent to give 3,4-bis(5-hexylthiophen-2-yl)furan-2,5-dione as a red oil (0.12 g, 25% yield). ^{1}H NMR (400 MHz, $CDCl_3$) δ 7.85 (d, 2H, J = 4.5 Hz), 6.87 (d, 2H, J = 4.5 Hz), 2.88 (t, 4H, J = 8.0 Hz), 1.72 (m, 4H), 1.32–1.41 (m, 12H), 0.90 (t, 6H, J = 7.0 Hz); ^{13}C NMR (100 MHz, $CDCl_3$) δ 164.7, 154.1, 133.1, 127.2, 126.3, 125.4, 31.5, 31.4, 30.4, 28.8, 22.6, 14.1; anal. calcd. for $C_{24}H_{30}O_3S_2$: C, 66.94; H, 7.02. Found: C, 66.79; H, 6.85;IR (ATR-FTIR): 1825, 1760 cm^{-1} (—C(O)OC(O)—).

4.2.8. Synthesis of 3,4-bis(5-dodecylthiophen-2-yl)furan-2,5-dione (C12-Th2MA)

A solution of dimethyl 2,3-bis(5-dodecylthiophen-2-yl)fumarate (**3b**) (0.30 g, 0.46 mmol), potassium hydroxide (0.48 g, 8.62 mmol) in ethanol:water (22:3 ml) solvent mixture was refluxed at 105 °C for 16 h. The reaction mixture was then allowed

to cool to room temperature, and then acidified to "pH 0–1" by HCl (3 M, 5 ml). The product was extracted from the resulting orange-red mixture by using chloroform. The resulting organic phase was washed with water, dried with Na_2SO_4, filtered, and evaporated to dryness to give a crude product. The crude product was purified by column chromatography on silica gel using chloroform as the eluent to give 3,4-bis(5-dodecylthiophen-2-yl)furan-2,5-dione as a red oil product (0.10 g, 35% yield). ^{1}H NMR (400 MHz, $CDCl_3$) δ 7.85 (d, 2H, J = 4.0 Hz), 6.86 (d, 2H, J = 4.0 Hz), 2.87 (t, 4H, J = 8.0 Hz), 1.71 (m, 4H), 1.25–1.40 (m, 36H), 0.89 (t, 6H, J = 7.0 Hz); ^{13}C NMR (100 MHz, $CDCl_3$) δ 164.7, 154.0, 133.1, 127.3, 126.3, 125.4, 31.9, 31.4, 30.4, 29.7, 29.6, 29.6, 29.5, 29.4, 29.3, 29.1, 22.7, 14.1; anal. calcd. for $C_{36}H_{54}O_3S_2$: C, 72.19; H, 9.09. Found: C, 72.42; H, 9.14; IR (ATR-FTIR), 1825, 1760 cm^{-1} (—C(O)OC(O)—); m.p. 54–55 °C.

4.2.9. Synthesis of dimethyl 2,3-diphenylfumarate (4)

Bis(triphenylphosphine)palladium(II) dichloride (0.116 g, 0.17 mmol) was added to a solution of phenyltrimethylstannane (2.0 g, 8.34 mmol) and dimethyl 2,3-dibromofumarate (1.0 g, 3.33 mmol) in anhydrous THF (15 ml). The reaction mixture was heated at 105 °C for 2 days. The reaction was followed by thin-layer chromatography. After the reaction is completed, the reaction mixture was concentrated on the rotary evaporator to give a dark crude semi-solid. The crude product was purified by column chromatography on silica gel using chloroform as the eluent to give dimethyl 2,3-diphenylfumarate as an off-white solid (0.916 g, 93% yield) ^{1}H NMR(400 MHz, $CDCl_3$) δ 7.40 (m, 5H), 3.56 (s, 3H). ^{13}C NMR(100 MHz, $CDCl_3$) δ 168.5, 137.6, 135.4, 128.8, 128.5, 128.1, 127.9, 52.3. m.p. 137–138 °C.

4.2.10. Synthesis of 2,3-diphenylfumaric acid (5)

A solution of dimethyl 2,3-diphenylfumarate (**4**) (0.285 g, 0.96 mmol) and potassium hydroxide (0.65 g, 11.6 mmol) in ethanol:water (30:4.5 ml) solvent mixture was refluxed at 105 °C for 16 h. The reaction mixture was then allowed to cool to room temperature, ethanol is removed in the rotary evaporator, and then acidified to "pH 0–1" by HCl (3 M, 2 ml) to give a white precipitate. The precipitate was filtered through buchner funnel, washed with water and dried under vacuum (~100 mTorr) to yield 2,3-diphenylfumaric acid as a white solid (0.17 g, 66.7% yield). ^{1}H NMR(400 MHz, $CDCl_3$) δ 13.21 (s, 1H), 7.40 (m, 5H); ^{13}C NMR (100 MHz, $CDCl_3$) δ 169.7, 136.4, 136.2, 129.0, 128.9, 128.2, 100.6; m. p. 273–274 °C.

4.3. Fabrication and characterization

The absorbance and emission characterizations have been carried out using Cary 100-UV–vis and Cary Eclipse, respectively (2.1×10^{-5} M). The electroluminesence spectrum has been collected using StellarNet Spectrometer with blue LED driven with Keithley 2400 Sourcemeter.

5. Supplementary data

Computed UV–vis Spectra of M1 and M2 (Fig. S1). Accelerated Luminescence Stability Test of C12-Th2MA (Fig. S2). ^{1}H and ^{13}C NMR Spectra of Compounds 3a, 3b, 4, 5, C6-Th2MA and C12-Th2MA (Fig. S3–S14). IR spectra of C12-Th2MA (Fig. S15).

Acknowledgments

H.U. and E.M. acknowledge support from The Science Academy, Young Scientist Award (BAGEP). H.U. acknowledges support from AGU-BAP (FOA-2015-24) and TUBITAK 113C021. E.M acknowledges support from AGU-BAP (FAB-2015-10), TUBITAK 5140079 and TUBITAK 114E107.

Appendix A. Supplementary data

Supplementary data associated with this article can be found, in the online version, at http://dx.doi.org/10.1016/j.synthmet.2015.09.027.

References

[1] P. Moreau, F. Anizon, M. Sancelme, M. Prudhomme, C. Bailly, C. Carrasco, M. Ollier, D. Severe, J.F. Riou, D. Fabbro, T. Meyer, A.M. Aubertin, J. Med. Chem. 41 (1998) 1631.
[2] N. Nakamura, A. Hirakawa, J.-J. Gao, H. Kakuda, M. Shiro, Y. Komatsu, C. Sheu, M. Hattori, J. Nat. Prod. 67 (2004) 46.
[3] X. Chen, Y. Zheng, Y. Shen, Chem. Rev. 107 (2007) 1777.
[4] N. Ferri, E.M. Beccalli, A. Contini, A. Corsini, M. Antonino, T. Radice, G. Pratesi, S. Tinelli, F. Zunino, M.L. Gelmi, Bioorg. Med. Chem. 16 (2008) 1691.
[5] N. Ferri, T. Radice, M. Antonino, E.M. Beccalli, S. Tinelli, F. Zunino, A. Corsini, G. Pratesi, E.M. Ragg, M.L. Gelmi, A. Contini, Bioorg. Med. Chem. 19 (2011) 5291.
[6] W. Steglich, B. Steffan, L. Kopanski, G.E. Eckhardt, Angew. Chem. Int. Ed. Eng. 19 (1980) 459.
[7] U. Zehavi, J. Org. Chem. 42 (1977) 2819.
[8] M. Pawlowska, J. Zukowski, D.W. Armstrong, J. Chromatogr. A 666 (1994) 485.
[9] A. Micó-Tormos, F. Bianchi, E.F. Simó-Alfonso, G. Ramis-Ramos, J. Chromatogr. A 1216 (2009) 3023.
[10] Q. Guan, D. Zuo, N. Jiang, H. Qi, Y. Zhai, Z. Bai, D. Feng, L. Yang, M. Jiang, K. Bao, C. Li, Y. Wub, W. Zhang, Bioorg. Med. Chem. Lett. 25 (2015) 631.
[11] C. Peifer, T. Stoiber, E. Unger, F. Totzke, C. Schächtele, D. Marmé, R. Brenk, G. Klebe, D. Schollmeyer, G. Dannhardt, J. Med. Chem. 49 (2006) 1271.
[12] D. Wutz, C. Falenczyk, N. Kuzmanovic, B. König, RSC Adv. 5 (2015) 18075.
[13] M.M. Krayushkin, V.N. Yarovenko, S.L. Semenov, V.Z. Shirinyan, A. Yu Martynkin, B.M. Uzhinov, Russ. J. Org. Chem. 38 (2002) 1331.
[14] V.Z. Shirinyan, M.M. Krayushkin, L.I. Belen'kii, A.A. Shimkin, A. YuMartynkin, B. M. Uzhinov, Russ. J. Org. Chem. 38 (2002) 1335.
[15] S. Reineke, F. Lindner, G. Schwartz, N. Seidler, K. Walzer, B. Lüssem, K. Leo, Nature 459 (2009) 234.
[16] Q. Wang, D. Ma, Chem. Soc. Rev. 39 (2010) 2387.
[17] C. Shena, Y. Yang, S. Jin, J. Ming, H. Feng, Z. Xu, Optik 121 (2010) 1487.
[18] S. Park, J.E. Kwon, S.H. Kim, J. Seo, K. Chung, S.-Y. Park, D.-J. Jang, B.M. Medina, J. Gierschner, S.Y. Park, J. Am. Chem. Soc 131 (2009) 14043.
[19] J.A. Degheili, R.M. Moustafa, D. Patra, B.R. Kaafarani, J. Phys. Chem. A 113 (2009) 1244.
[20] E.M. Beccalli, M.L. Gelmi, A. Marchesini, Eur. J. Org. Chem. 1999 (1999) 1421.
[21] A. El Yahyaoui, G. Felix, A. Heynderickx, C. Moustrou, A. Samat, Tetrahedron 63 (2007) 9482.
[22] M. Dubernet, V. Caubert, J. Guillard, M.-C. Viaud-Massuard, Tetrahedron 61 (2005) 4585.
[23] M1 (3,4-diphenyl-2,5-furandione) is commerically available from Sigma–Aldrich under the product number: 43095 (CAS Number: 4808-48-4).
[24] H. Usta, M.D. Yilmaz, A.-J. Avestro, D. Boudinet, M. Denti, W. Zhao, J.F. Stoddart, A. Facchetti, Adv. Mater. 25 (2013) 4327.
[25] H. Usta, G. Lu, A. Facchetti, T.J. Marks, J. Am. Chem. Soc. 128 (2006) 9034.
[26] Y. Pocker, M.J. Hill, J. Am. Chem. Soc. 93 (1971) 691.
[27] B.S. Furniss, A.J. Hannaford, P.W.G. Smith, A.R. Tatchell, Vogel's Textbook of Practical Organic Chemistry, 5th ed., Longman, Harlow, 1989 (ISBN 0-582-46236-3).
[28] H. Usta, C. Risko, Z. Wang, H. Huang, M.K. Deliomeroglu, A. Zhukhovitskiy, A. Facchetti, T.J. Marks, J. Am. Chem. Soc. 131 (2009) 5586.
[29] J.W. Eastman, Photochem. Photobiol. 6 (1967) 55.
[30] I.B. Berlaman, Fluorescence Spectra of Aromatic Molecules, Academic Press, New York, 1971.
[31] N.J. Turro, Modern Molecular Photochemistry, University Science Books, Sausalito, CA, 1991.
[32] C.-Y. Sun, X.-L. Wang, X. Zhang, C. Qin, P. Li, Z.-M. Su, D.-X. Zhu, G.-G. Shan, K.-Z. Shao, H. Wu, J. Li, Nat. Commun. 4 (2013) 2717.
[33] Anant A. Setlur, Electrochem, Soc. Interface 16 (2009) 32–36.
[34] T. Erdem, H.V. Demir, Nat. Photon. 5 (2011) 126.
[35] G. Wyszecki, W.S. Stiles, Color Science: Concepts and Methods, Quantitative Data and Formulae, Wiley-Interscience, 2000.
[36] E. Jang, S. Jun, H. Jang, J. Lim, B. Kim, Y. Kim, Adv. Mater. 22 (2010) 3076–3080.
[37] S. Su, W. Liu, R. Duan, L. Cao, G. Su, C. Zhao, J. Alloys Compd. 575 (2013) 309–313.